J|A|C|S
COMMUNICATIONS

Published on Web 08/12/2008

Dissecting Entropic Coiling and Poor Solvent Effects in Protein Collapse

Frauke Gräter,*,†,‡,|| Pascal Heider,§ Ronen Zangi,† and B. J. Berne†

Department of Chemistry, Department of Biology, and Department of Applied Physics and Applied Mathematics, Columbia University, 3000 Broadway, New York, New York 10027

Received April 30, 2008; E-mail: frauke@picb.ac.cn

Protein folding to specific functional structures is preceded by a largely unspecific protein collapse into a molten globule state which reflects protein elasticity. Contributions to protein elasticity, however, are not yet well understood. Experimental measurements on single protein chains using force spectroscopy reveal a force−extension behavior in reasonable agreement with polymer random coil models such as the worm-like chain model (WLC).[1] WLC fits to such data yield an effective persistence length in the range $p_{eff} = 0.3-0.6$ nm (Figure 1a)[2,3] as a measure of protein elasticity, in agreement with end-to-end distances of loops in protein structures.[4] Surprisingly, recent measurements at low force again do not reveal any departure from purely entropic chain behavior.[5] Consequently, a major effort has been focused on the development of theories for protein elasticity solely based on chain entropy,[6,7] with departures from entropic coiling behavior only considered at high force in the form of enthalpic stretching.[8,9] The apparent random coil behavior, however, is not in agreement with the common notion of protein hydrophobic collapse. Protein unfolding involves exposure of hydrophobic side chains buried in the protein core of the folded state, and hence, water is a poor solvent for unfolded or disordered proteins.[10] Recent FRET,[11] AFM,[2] or NMR experiments[12] reveal signatures for hydrophobic collapse in primary refolding events. Poor solvent conditions drastically change the equilibrium and dynamical properties of polymers[13,14] and also entail pronounced deviations from random coil stretching behavior, as predicted[15,16] and recently shown by AFM studies of polystyrene.[17]

We aim to resolve the contradiction between the hydrophobic nature of unfolded proteins and their apparent worm-like chain behavior. To assess the entropic chain contribution to protein elasticity, which corresponds to the coiling behavior of a protein in a good solvent (gs), we employ an all-atom random coil model of the protein ubiquitin[18] using a modified force field, in which only bonded interactions and the repulsive part of the Lennard−Jones interactions (C12) were kept. This entropic chain incorporates the correct volume exclusion, backbone geometry, and conformational freedom of the protein and ignores nonlocal interactions and solvent-induced effects. It therefore corresponds to an unfolded protein chain in an optimal solvent. The force−extension curve of this model, determined from MD simulations, closely follows WLC behavior, with a persistence length of $p_{gs} = 1.2$ nm, a finding remarkably sequence-independent (Suppl. Figure 1). In this particular context, we refer to this chain as a "stiff chain" because it has a persistence length roughly three times larger than the commonly assumed values (Figure 1a). Given the rigidity of the π-conjugated amide bond and the restriction of the two remaining dihedrals to a specific region on the Ramachandran plot, the obtained persistence length of approximately three amino acids in length is very reasonable.[13,19] It is also in quantitative agreement with recent findings for unfolded proteins[11,20] and with the high population of extended conformations expected in the absence of nonlocal interactions and secondary structure.[21]

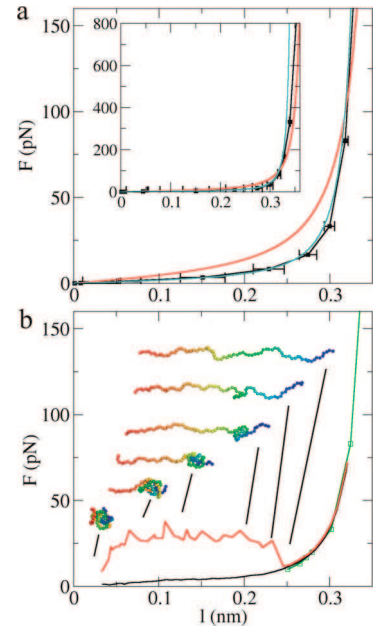

Figure 1. Force−extension behavior in good and poor solvents. (a) For a protein in a good solvent obtained from all-atom simulations of ubiquitin as an entropic chain (black). A WLC fit gives a persistence length of $p_{gs} = 1.2$ nm (cyan), remarkably different to a WLC with $p_{eff} = 0.4$ nm experimentally found (red). (b) For a protein in a poor solvent obtained for a coarse-grained (bead−spring model) hydrophobic chain (red), in comparison to the dwell length of the same model under force−clamp (green, compare Suppl. Figure 3) and to good solvent conditions (black). l is the average length per residue.

To clarify the role of poor-solvent effects, a simplified coarse-grained model of a protein-like entropic chain was employed consisting of 76 spheres at the positions of C-α atoms of ubiquitin (0.5 nm in diameter) connected by springs, with angle restraints chosen to give the backbone stiffness of ubiquitin. The force−extension behavior of this chain in a poor solvent was calculated by adding an effective pairwise interaction potential to mimic the hydrophobic effect, estimated from the attraction between small hydrophobic spheres in water (Figure 1b). At low to intermediate end-to-end distances of the chain, some of the spheres are involved in forming a globule via nonlocal contacts, and extension requires ∼20 pN to enforce a continuous globule-to-coil transition. For extensions larger than l ∼0.23 nm, the hydrophobic chain shows the same force−extension behavior as the purely entropic chain, since the penalty for chain bending then exceeds the benefit from contact formation. An analytical derivation of the stretching response of

† Department of Chemistry.
‡ Department of Biology.
§ Department of Applied Physics and Applied Mathematics.
|| Current address: MPG-CAS Partner Institute for Computational Biology, 320 Yueyang Lu, Shanghai.

10.1021/ja802341q CCC: $40.75

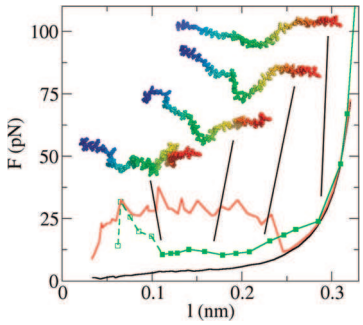

Figure 2. Force extension behavior for a protein chain in poor solvent, for which the hydrophobic attractions between residues are assigned to the side chains (green). This model shows moderate deviation from the entropic chain (dashed black) for $l > 0.1$ nm.

worm-like chains in poor solvents (Supporting Information (SI) and Suppl. Figure 2) confirmed this finding in that no significant contraction of the poorly solvated chain over the noninteracting chain was observed in this regime. We expect the hump-like profile to be a characteristic of a polymer in a poor solvent, when the length scale of the attractive forces (~1 nm) is similar or smaller than the persistence length (1.2 nm), i.e. for relatively stiff chains. As expected, the drop in force at medium extension and the resulting hump disappear for a softer polymer ($p_{gs} = 0.4$ nm) in a poor solvent, modeled here by omitting angle constraints in the coarse-grain model (Suppl. Figure 4). The force plateau directly passes into the entropic chain behavior, since nonlocal contact formation is not hampered by bending rigidity even for large chain extensions. A plateau[15,16] for flexible chains and a hump-like shape for comparably stiff chains have been predicted theoretically[22] and have been found in force spectroscopy measurements of single hydrophobic polymer chains in water.[17]

Proteins are stiff polymers ($p_{gs} = 1.2$ nm) in poor solvents, yet their experimental force−extension behavior does not exhibit a hump but instead approximately follows an apparent worm-like chain behavior. As an important feature of proteins and a possible explanation for this discrepancy, hydrophobic forces are expected to be strongest between the protein's hydrophobic side chains. To investigate the effect of side chains, we determined the force−extension profile of an all-atom protein chain in which pairwise attractions are exclusively assigned to the side chains (Figure 2, green curve; see SI for details). As expected, interside chain interactions endure up to significantly larger extensions, as reflected by an offset in force from the respective behavior in good solvent up to $l = 0.30$ nm. The attractive side chain interactions thus allow proteins in poor vs good solvents appear softer, instead of causing the pronounced hump of other stiff polymers. Our simple model with hydrophobic interactions also quantitatively captures the major features of protein collapse in water after force quench as observed by force spectroscopy,[23,18] namely the average dwell length (0.8 of the 100 pN length at 10 pN) and the high cooperativity of the coil-to-globule transition (Figure 1b and Suppl. Figure 3).

Our study suggests that the persistence length commonly used to analyze AFM force−extension data reflects an effective protein elasticity incorporating entropic as well as attractive interactions, most likely of hydrophobic nature, which lower the persistence from $p_{gs} = 1.2$ nm to $p_{eff} \sim 0.6$ nm measured in water.[11,5] The low force regime ($F < 20$ pN) is dominated by nonlocal, supposedly hydrophobic interactions, while in the high force regime stiff entropic chain behavior and enthalpic stretching are dominant. According to our model, the strong hydrophobic effect in water compacts an unfolded protein against its bending rigidity. The high chain stiffness combined with solvent mediated attraction between side chains consequently results in a force−extension behavior pronouncedly different from the plateau (Suppl. Figure 4) found for the relatively flexible polystyrene chains in water[17] or the hump-like behavior (Figure 1) found for simple stiff chains.[22] We thus find that the incorporation of a correct entropic chain persistence into coarse-grain models frequently used for collapse and folding simulations is crucial,[24,25] while the details of a chosen elasticity theory to describe protein collapse (worm-like chain versus freely rotating chain) is of minor importance, because the dominant contributions are not due to chain entropy. The recent advances in force spectroscopy studies in conjunction with solvent dependency of protein collapse will help test our predictions.

Acknowledgment. We thank Julio Fernandez, Dave Thirumalai, Greg Morrison, Eric Siggia, and Alfredo Alexander-Katz for many fruitful discussions. F.G. was supported by a Columbia University grant. B.J.B.; F.G. and P.H. were also supported by the Alexander von Humboldt Foundation.

Supporting Information Available: Supplementary force−extension curves, collapse trajectories, derivation of a modified worm-like chain formulation, and simulation methods.This material is available free of charge via the Internet at http://pubs.acs.org.

References

(1) Marko, J. F.; Siggia, E. D. *Macromolecules* **1995**, *28*, 8759–8770.
(2) Rief, M.; Gautel, M.; Oesterhelt, F.; Fernandez, J. M.; Gaub, H. E. *Science* **1997**, *276*, 1109–1112.
(3) Dietz, H.; Berkemeier, F.; Bertz, M.; Rief, M. *Proc. Natl. Acad. Sci. U.S.A.* **2006**, *103*, 12724–12728.
(4) Zhou, H. X. *Biochemistry* **2004**, *43*, 2141–2154.
(5) Schlierf, M.; Berkemeier, F.; Rief, M. *Biophys. J.* **2007**, *93*, 3989–3998.
(6) Seyed-allaei, H. *Phys. Rev. E* **2005**, *72*, 41908.
(7) Toan, N. M.; Marenduzzo, D.; Micheletti, C. *Biophys. J.* **2005**, *89*, 80–86.
(8) Hugel, T.; Rief, M.; Seitz, M.; Gaub, H. E.; Netz, R. R. *Phys. Rev. Lett.,* **2005**, *94*, 48301.
(9) Janshoff, A.; Neitzert, M.; Oberdorfer, Y.; Fuchs, H. *Angew. Chem., Int. Ed.* **2000**, *39*, 3213–3237.
(10) Vitalis, A.; Wang, X.; Pappu, R. V. *Biophys. J.* **2007**, *93*, 1923–1937.
(11) Schuler, B. *ChemPhysChem,* **2005**, *6*, 1206–1220.
(12) Mok, K. H.; Kuhn, L. T.; Goez, M.; Day, I. J.; Lin, J. C.; Andersen, N. H.; Hore, P. J. *Nature* **2007**, *447*, 106–109.
(13) Flory P. J. *Statistical Mechanics of Chain Molecules*; Interscience: New York, 1969.
(14) Halperin, A.; Goldbart, P. M. *Phys. Rev. E* **2000**, *61*, 565–573.
(15) Halperin, A.; Zhulina, E. B. *Europhys. Lett.* **1991**, *16*, 337–341.
(16) Morrison, G.; Hyeon, C.; Toan, N. M.; Ha, B. Y.; Thirumalai, D. *Macromolecules* **2007**, *40*, 7343–7353.
(17) Gunari, N.; Balazs, A. C.; Walker, G. C. *J. Am. Chem. Soc.* **2007**, *129*, 10046.
(18) Walther, K. A.; Grater, F.; Dougan, L.; Badilla, C. L.; Berne, B. J.; Fernandez, J. M. *Proc. Natl. Acad. Sci. U.S.A.* **2007**, *104*, 7916–7921.
(19) Livadaru, L.; Netz, R. R.; Kreuzer, H. J. *Macromolecules* **2003**, *36*, 3732–3744.
(20) Danielsson, J.; Andersson, A.; Jarvet, J.; Graslund, A. *Magn. Reson. Chem.* **2006**, *44*, S114–S121.
(21) Chen, K.; Liu, Z.; Zhou, C.; Bracken, W. C.; Kallenbach, N. R. *Angew. Chem., Int. Ed.* **2007**, *46*, 9036–9039.
(22) Rosa, A.; Marenduzzo, D.; Kumar, S. *Europhys. Lett.* **2006**, *75*, 818–824.
(23) Garcia-Manyes, S.; Brujic, J.; Badilla, C. L.; Fernandez, J. M. *Biophys. J.* **2007**, *93*, 2436–2446.
(24) Ueda, Y.; Taketomi, H.; Gō, N. *Biopolymers* **1978**, *17*, 1531–1548.
(25) Cheung, M. S.; Garcia, A. E.; Onuchic, J. N. *Proc. Natl Acad. Sci. U.S.A.* **2002**, *99*, 685–690.

JA802341Q

Dissecting entropic coiling and poor solvent effects in protein collapse, F. Gräter et al.: Supplementary information

Methods

All-atom simulations of a protein entropic chain: All simulations were carried out using the MD software package GROMACS 3.1.4 (1). The OPLS/AA force field (6) was used. An all-atom model of ubiquitin and the OPLS/AA force field (2) were used, as previously described (3).

To examine the force-extension behavior of ubiquitin due to chain entropy, we performed MD simulations of an all atom model of ubiquitin with a modified force field in which only bonded interactions (bond, angle, and dihedral terms) and the repulsive part of the Lennard-Jones interactions (C12) were kept. Partial charges and the attractive contribution to the Lennard-Jones interactions between all atoms of the protein were set to zero. The effect of solvent is not included in this model. This resulted in a system modeling ubiquitin as a purely entropic chain, in which the conformational ensemble is only restricted by the bonded interactions, mainly the dihedral potentials along the protein backbone, and by the local steric repulsion of the atom spheres.

To examine solvent effects on chain folding in poor solvents like water a very simple coarse-grain model was devised based on the coiling behavior observed for the all-atom model in solvent. The energy function of the coarse-grain model is given by

$$E_{\text{entropic}} = E_{\text{b}} + E_{\text{a}} + E_{\text{LJ}} \quad (1)$$

$$= \frac{1}{2}k_{\text{b}}(l - l_0)^2 + \frac{1}{2}k_{\text{a}}(\theta - \theta_0)^2 + \frac{C_{12}}{r^{12}} \quad (2)$$

Each amino-acid is represented by a single sphere on the position of the C-α atoms. The spheres were connected with bonds of length $l_0 = 0.38\,\text{nm}$, the distance between C-α in experimental protein structures, with a stiffness of $k_{\text{b}} = 10^7$ kJ/mol/nm^2. The equilibrium angle θ_0 was chosen such that the all-atom force-extension profile was recovered. For an estimate of the average pairwise hydrophobic force between two hydrophobic side chains, we performed a potential-of-mean force (PMF) calculation for two spherical solutes in explicit water (SPC/E), using values $\epsilon = 4\,\text{kJ/mol}$ and $\sigma = 0.5\,\text{nm}$ typical for leucine residues. The PMF is shown

in Supplementary Fig. 5. The PMF was approximated by a Lennard Jones potential, with $\epsilon = 1.9\,\mathrm{kJ/mol}$ and $\sigma = 0.5\,\mathrm{nm}$. Of course a pairwise summation of two-body pmfs equivalent to the superposition approximation is not accurate, nevertheless we expect this to provide some insight into the solvent effect especially for extended chain states in a poor solvent such as water. We tested the influence of the desolvation barrier found for hydrophobic contacts by directly using the PMF as shown in the coarse-grained simulations, but did not find a significant change in the equilibrium force-extension behavior (not shown).

We note that this coarse-grain model lacks the significant flexibility of side chains to form hydrophobic contacts in fairly extended chain conformations. To account for this, we also employed a model for a protein in poor solvent on the basis of the all-atom model for an entropic chain (see above). We included the Lennard-Jones attractive term (C6) for all atoms of the side chains, resulting in a chain, in which the extent of entropic coiling is maintained, but attractive sidechain interactions added. Due to the simplicity this model can not be expected to yield realistic conformations of highly coiled states, but can account for the effect of inter-sidechain interaction in the stretched state.

Both the all-atom and the coarse-grained model, as entropic chains or as hydrophobic chain in poor solvent, were subjected to umbrella sampling using Brownian dynamics simulations. Umbrella potentials were applied to the terminal C-α atoms, using a spring constant of $k_\mathrm{U} = 100\,\mathrm{kJ/mol/nm^2}$. From each simulation at a given position of the two umbrella potentials, the average force was calculated and is here shown as a function of end-to-end distance of the protein normalized by the number of C-α-C-α bonds. Weighted histogram analysis did not significantly improve the convergence of the mean force.

In analogy to force-quench experiments (4), we also carried out simulations of the entropic and hydrophobic coarse-grain model at a low constant force to monitor chain collapse. The chain was stretched at high force (500 pN) and then relaxed to a constant force of 10-20 pN. For the entropic chain, the obtained mean chain length is in close agreement with the force-extension behavior obtained from umbrella sampling (Fig. 1). The hydrophobic chain after relaxation shows coiling similar to the entropic chain, but subsequently a highly cooperative coil-to-globule transition, i.e. a transition of which the time scale is significantly shorter than the prior dwell time. The simulated trajectories are in close agreement with those obtained in force-clamp AFM experiments (4; 5) with respect to the average chain length of the coiled state ($l = 0.26\,\mathrm{nm}$), and the range of forces at which the transition between the coil and globular state occurs (10-20 pN range). Thus, our hydrophobic chain model captures the crucial factors driving collapse of the polymer, namely the entropic

chain persistance and the overall attraction of the united atom side chains in a poor solvent.

Modification of the worm-like chain model in poor solvent conditions and strong-stretching behaviour

We present a modified worm-like chain description of chains folding under poor solvent conditions. Our approach is similar to the one used by Marko and Siggia (6) to incorporate electrostatic repulsion of negatively charged phosphate groups into a worm-like chain model of DNA in dilute electolytes. Here, we assume that the segments along the chain attract each other because of the hydrophobic effect through a Lennard-Jones attraction, as was done in the above coarse grained model,

$$V(\|\mathbf{r}(s)-\mathbf{r}(s')\|)-V(|s-s'|)=\frac{-C_6}{\|\mathbf{r}(s)-\mathbf{r}(s')\|^6}-\frac{-C_6}{|s-s'|^6}, \tag{3}$$

where $\mathbf{r}(s)$ is the position of the chain segment s in space and $C_6 := 4\epsilon\sigma^6$, where ϵ and σ are the LJ parameters. Since coiling is driven by the change in energy relative to the fully stretched state, we have to substract the potential energy $V(|s-s'|)$ of the stretched chain.

To study the strong-stretching behaviour we make a Gaussian approximation of (3), cf. (7). For a strong applied force the displacement of the chain orthogonal to the direction of the force is a small quantity, so that in the Gaussian approximation we assume that the norm $\|\mathbf{t}_\perp(s)\|^2$ of that orthogonal component of the tangent vector $\mathbf{t}(s) = \partial_s\mathbf{r}(s)$ is small. Moreover, in this approximation we find that the curvature of the chain $\kappa(s)$ satisfies

$$\kappa(s)^2 = \|\partial_s\mathbf{t}_\perp(s)\|^2 \tag{4}$$

to quadratic order and we obtain (7),

$$\|\mathbf{r}(s)-\mathbf{r}(s')\|^2 = |s-s'|^2\left(1-\frac{(s-s')^2\|\partial_s\mathbf{t}_\perp(s')\|^2}{12}\right)+O(\|\partial_s\mathbf{t}_\perp(s')\|^4). \tag{5}$$

If we plug this into Eq. (3) and expand in terms of $\|\partial_s\mathbf{t}_\perp(s)\|^2$ we obtain

$$V(\|\mathbf{r}(s)-\mathbf{r}(s')\|)-V(|s-s'|) = -\frac{C_6}{4}\frac{\|\partial_s\mathbf{t}_\perp(s')\|^2}{|s-s'|^4}+O(\|\partial_s\mathbf{t}_\perp(s)\|^4). \tag{6}$$

This approximation is only valid in the strong-stretching regime, when $\|\mathbf{t}_\perp(s)\|^2$ is a small quantity.

The double integral over the total chain length L,

$$E_{add} = \frac{1}{2}\int_0^L \int_0^L V(\|\mathbf{r}(s) - \mathbf{r}(s')\|) - V(|s - s'|)dsds', \tag{7}$$

gives the total additional energy of the worm-like chain due to poor solvent effects and corrects the Fixman-Kovac bending energy including these additional effects. The energy is then given by

$$\frac{E}{k_B T} = \int_0^L \frac{p\kappa^2}{2}ds - fz + E_{add}, \tag{8}$$

where p is the persistence length and $f = F/(k_B T)$ is the applied force in reduced units. The equilibrium extension can be computed using the Boltzmann distribution and the equipartition theorem as outlined in (6). For this we need to compute the Fourier transform of the integrals in (8), where the integrands have been replaced by their Gaussian approximations (4) and (6). The Fourier transform ($\tilde{f}(q) = \int e^{-iqs} f(s)ds$) is found to be

$$\frac{E}{k_B T} = \frac{1}{2}\int_0^{2\pi} \left[(p + K(q))\, q^2 + f\right] \|\widetilde{\mathbf{t}_\perp}(q)\|^2 \frac{dq}{2\pi} - fL, \tag{9}$$

where the kernel $K(q)$ is defined by

$$K(q) := -\frac{C_6 \pi}{12} q^3. \tag{10}$$

By means of the equipartition theorem ((6)) we determine the force-extension relationship

$$\frac{z}{L} = 1 - \frac{1}{2\pi}\int_0^{2\pi} \left[pq^2 + K(q)q^2 + f\right]^{-1} dq, \tag{11}$$

where z is the length of the chain along the direction in which the force f is applied.

Eq.(11) differs from the original worm-like chain formulation by having the $K(q)q^2$ term in the denominator of the integrand. This effectively reduces the chain length z to an extent depending on the strength of the attractive interaction, as given by C_6. This is the result expected for attractive potentials $V(r) < 0$, and is the opposite effect found in a repulsive chain such as the polyelectrolyte DNA (6). The overall effect for chain reduction, according to this model, however, is small. For a reasonable range of C_6, defined as $C_6 = \epsilon\sigma^6$, with $\epsilon = 2\,\text{kJ/mol}$ and $\sigma = 0.4\,\text{nm}$, z decreases not more than $\sim 2\,\%$ in the relevant force range ($pF > k_B T$), as shown in Supplementary Fig. 2. Thus, for the high stretching regime, no significant chain contraction due to the hydrophobic effect should be expected.

References

[1] E. Lindahl, B. Hess, and D. van der Spoel, *J. Mol. Model.*, **2001**, *7*, 306–317.

[2] W. L. Jorgensen and J. Tirado-Rives, *J. Am. Chem. Soc.*, **1988**, *110*, 1657–1666.

[3] K. Walther, F. Gräter, L. Dougan, B. J. Berne, and J. Fernandez, *Proc. Natl. Acad. Sci. USA*, **2007**, *104*, 7916–7921.

[4] J. M. Fernandez and H. B. Li, *Science*, **2004**, *303*, 1674–1678.

[5] S. Garcia-Manyes, J. Brujic, C. L. Badilla, and J. M. Fernandez, *Biophys. J.*, **2007**, *93*, 2436–2446.

[6] J. F. Marko and E. D. Siggia, *Macromolecules*, **1995**, *28*, 8759–8770.

[7] J. Skolnick and M. Fixman, *Macromolecules*, **1977**, *10*, 944.

Supplementary Figures

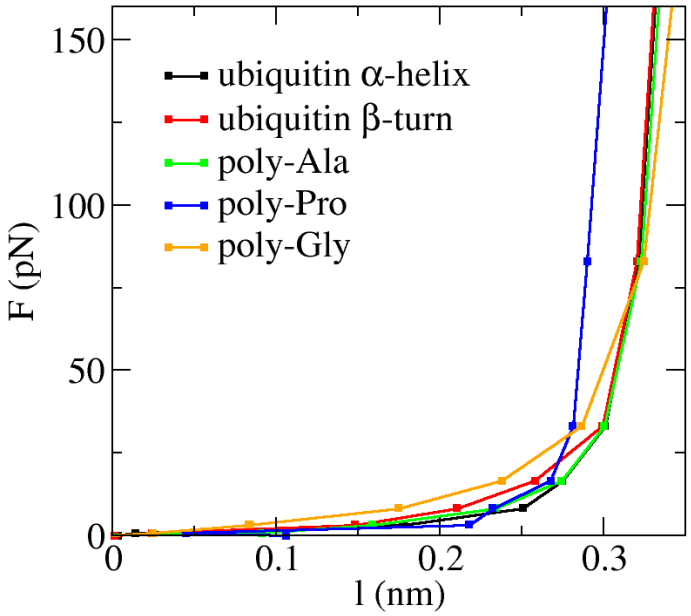

Supplementary Fig. 1: Force-extension behavior of protein entropic chains with different amino acid sequnces. Glycines (yellow) render a peptide more flexible due to the smaller steric hindrance, and prolines (blue), with only one dihedral degree of freedom, render a stiffer peptide than poly-alanine (green) or other naturally occurring peptides (red, black).

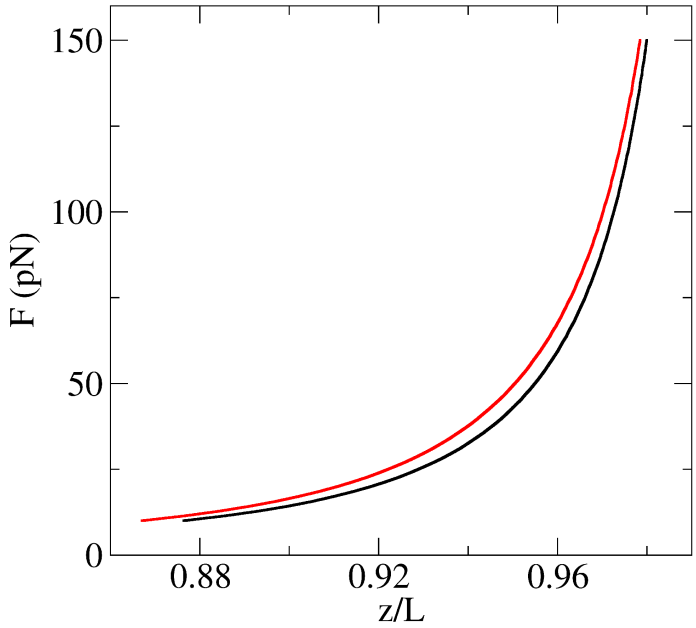

Supplementary Fig. 2: WLC force-extension profile obtained from Eq.(11) in the absence (black) and presence (red) of hydrophobic interactions ($C_6 = 0$ and $C_6 = 0.0081\,\mathrm{nm}^6$, corresponding to $\epsilon = 1.9\,\mathrm{kJ/mol}$, respectively). The increase in coiling due to the hydrophobically induced attractions is minor for the given persistence length of 1.2 nm of the WLC.

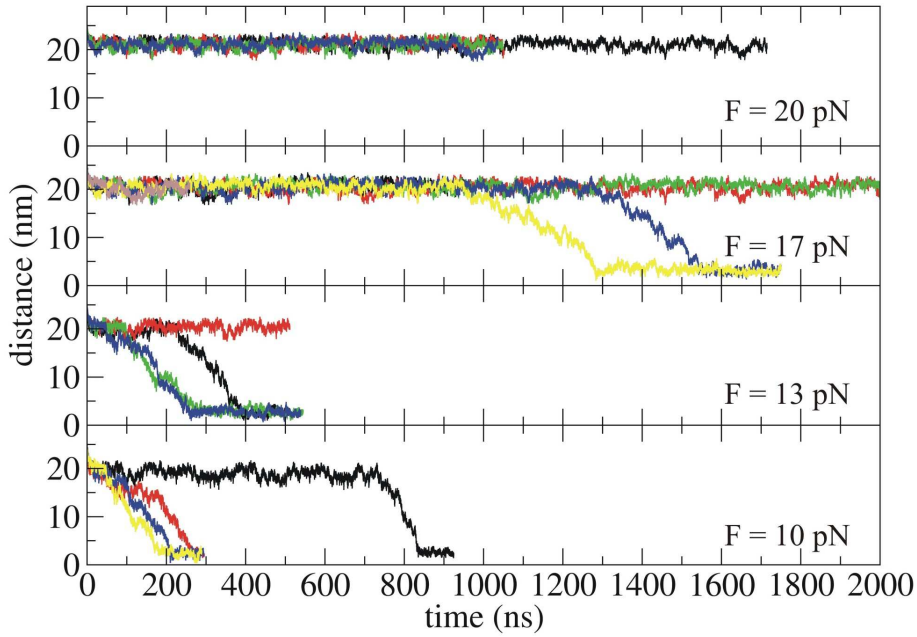

Supplementary Fig. 3: End-to-end distances of the chain over time during Brownian dynamics simulations and the hydrophobic model of the coarse-grained chain. After force quench to the force as indicated, the chain remained elongated and in the coiled state until a fast and cooperative collapse into the globular state occurs. Cooperativity here is measured by the time scale of the collapse transition itself relative to the dwell time, and was here found to be high, in agreement with experimental trajectories. Several simulations at the same external force and only differing by different seeds for random forces are shown.

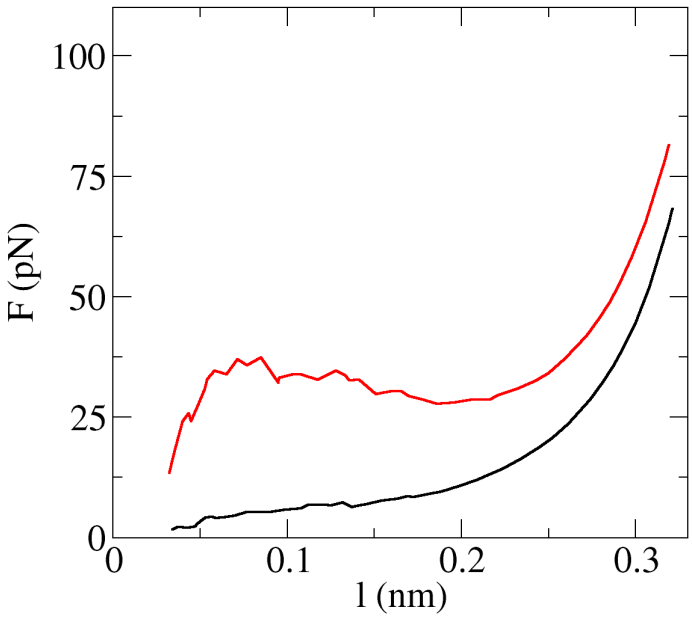

Supplementary Fig. 4: Force-extension behavior for a soft chain in poor (red) and good (black) solvent conditions, obtained for a coarse-grained hydrophobic and entropic chain, respectively (compare to the stiff chain in Fig. 1b).

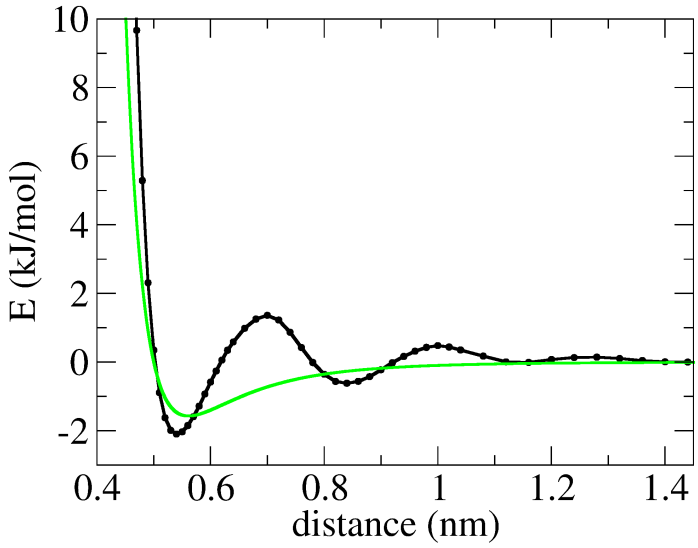

Supplementary Fig. 5: The Potential-of-mean-force (pmf) between two hydrophobic spheres in water obtained from MD simulations (black) on two LJ spheres in SPC/E water, and the Lennard Jones potential fit to the pmf used in the coarse-grain simulations to account for the hydrophobic effect (green).